

Small-Scale System for Evaluation of Stretch-Flangeability with Excellent Reliability

JAE IK YOON,¹ JAIMYUN JUNG,¹ HAK HYEON LEE,¹
and HYOUNG SEOP KIM^{1,2,3} 

1.—Department of Materials Science and Engineering, Pohang University of Science and Technology (POSTECH), Pohang 37673, Republic of Korea. 2.—Center for High Entropy Alloys, Pohang University of Science and Technology (POSTECH), Pohang 37673, Republic of Korea. 3.—e-mail: hskim@postech.ac.kr

We propose a system for evaluating the stretch-flangeability of small-scale specimens based on the hole-expansion ratio (HER). The system has no size effect and shows excellent reproducibility, reliability, and economic efficiency. To verify the reliability and reproducibility of the proposed hole-expansion testing (HET) method, the deformation behavior of the conventional standard stretch-flangeability evaluation method was compared with the proposed method using finite-element method simulations. The distribution of shearing defects in the hole-edge region of the specimen, which has a significant influence on the HER, was investigated using scanning electron microscopy. The stretch-flangeability of several kinds of advanced high-strength steel determined using the conventional standard method was compared with that using the proposed small-scale HET method. It was verified that the deformation behavior, morphology and distribution of shearing defects, and stretch-flangeability results for the specimens were the same for the conventional standard method and the proposed small-scale stretch-flangeability evaluation system.

INTRODUCTION

To address the trend towards more demanding environmental and safety regulations worldwide, the automobile industry has continued to reduce the weight of body-in-white components and to increase their stability by using more advanced high-strength steels (AHSS) for automotive components.¹ To satisfy these needs, types of AHSS with superior mechanical properties [e.g., dual-phase (DP) steel, transformation-induced plasticity (TRIP) steel, and twinning-induced plasticity (TWIP) steel] have been developed by many research groups.^{2–4}

Even though many studies have been conducted to develop AHSS with strength grade > 1 GPa for use in automotive components, it is difficult to utilize AHSS for automotive parts because their formability is limited, compared with that of conventional low-strength grade steels already used in automotive components.⁵ In particular, many failures occur during forming of automotive components because the stretch-flangeability (ability to

resist edge fracture during forming of complex automotive components) of AHSS is extremely limited.^{6,7} The stretch-flangeability limitation of AHSS has become a bottleneck in the design and manufacturing of automotive parts for lightweight bodyframes, and microstructural factors have been proposed to improve the stretch-flangeability of AHSS for better automotive applications.⁸ Therefore, it is particularly critical to evaluate and analyze the potential for better stretch-flangeability in development of AHSS for use in automotive parts.

Stretch-flangeability is measured using the hole-expansion test (HET). This is done according to the ISO 16630 standard evaluation method.⁹ The hole-expansion ratio (HER), measured using the HET, indicates the stretch-flangeability. However, the standard evaluation method requires an excessive number of test specimens in comparison with evaluation methods for other mechanical properties (e.g., tensile, compression, and bending tests). This means that it is difficult to evaluate the stretch-

flangeability of AHSS in the development rather than mass-production stage. In addition, with the current standard method, it is difficult to evaluate stretch-flangeability at small scale in the laboratory, or to evaluate localized areas of a sheet. Because of the problems mentioned above, evaluating and providing feedback on the stretch-flangeability of AHSS has become a time-consuming and costly problem.

To resolve the various issues mentioned above, we propose a new system for stretch-flangeability evaluation of small-scale specimens. The new system has excellent reproducibility, reliability, and economic efficiency without the disadvantage of a sample-size effect. Here, size effect means that the mechanical testing results obtained depend on the specimen size. It is well known that the specimen size effect creates the problem that small-scale testing results are not reliable.^{10–12} Therefore, the size effect should be considered when designing a reliable system for evaluating the stretch-flangeability of small-scale specimens.

In this paper, the proposed stretch-flangeability evaluation system is named the “proposed small-scale HET (pssHET) system” and the standard stretch-flangeability evaluation system established by ISO is named the “ISO standard-scale HET (isoHET) system.” The behavior of samples subjected to pssHETs and isoHETs was investigated using finite-element method (FEM) simulations. Also, the distribution of the shearing defects in the hole-edge region of the specimens was investigated using field-emission scanning electron microscopy (FE-SEM). Through the simulation and experimental results, we demonstrate that the results of the pssHET system exhibit the same excellent reproducibility and reliability as those of the isoHET system.

EXPERIMENTAL PROCEDURES

Materials

In this study, specimens of four different types of AHSS (TWIP1100, DP980, DP780, and TRIP780) were used to evaluate stretch-flangeability using the isoHET and the newly pssHET. The results from the two systems were compared. The AHSS specimens were fabricated at POSCO (Republic of Korea).

Design of Small-Scale HET System with Finite-Element Analysis

To prevent the sample size effect, the dimensions of the specimen to be subjected to the pssHET with the same deformation behavior as that indicated by the isoHET should be determined. Moreover, the ratio of sample thickness to grain size should be sufficiently large. In this study, deformation behavior results from both HETs were compared and

analyzed based on stress triaxiality.¹³ In addition, the HER of the same material was quite different according to the distribution of shearing defects in the initial hole-edge region of the specimen.^{14,15} Because this distribution is a critical extrinsic factor affecting the HER, the distribution of shearing defects in the initial hole-edge region of the pssHET specimen should be compared with that of the isoHET specimen.

To verify the similarity of the deformation behavior between the isoHET and pssHET, three-dimensional static elastoplastic FEM simulations were carried out using the commercial FEM package ABAQUS v6.9. The dimensions (e.g., specimen dimension, shape of the test dies) used in simulations of both HET systems were the same as those used in the experimental HETs. Eight-node fully integrated hexahedral elements (C3D8) were used, with at least five elements along the thickness direction of the specimen to analyze reasonable bending deformation behavior. The Young’s modulus and Poisson’s ratio were 210 GPa and 0.29, respectively. In this study, the stress–strain curve of TWIP1100 steel was used,¹⁵ the isotropic hardening with von Mises yield criterion was applied, and anisotropy and fracture models were not included. To analyze the deformation behavior observed during the HETs, the stress triaxiality parameter (TRIAx) was used, which is extensively used in literature on ductile fracture. The stress triaxiality was calculated using the following equation:¹³

$$\eta = \frac{\sigma_m}{\bar{\sigma}} \quad (1)$$

where σ_m and $\bar{\sigma}$ are the hydrostatic stress and von Mises equivalent stress, respectively. Here, σ_m and $\bar{\sigma}$ were calculated using the following equations:¹³

$$\sigma_m = \frac{1}{3}(\sigma_1 + \sigma_2 + \sigma_3) \quad (2)$$

$$\bar{\sigma} = \sqrt{\frac{1}{2}[(\sigma_1 - \sigma_2)^2 + (\sigma_2 - \sigma_3)^2 + (\sigma_3 - \sigma_1)^2]} \quad (3)$$

where σ_1 , σ_2 , and σ_3 denote principal stresses.

In addition, the sheared surfaces in the hole-edge region of specimens subjected to the two HET methods were observed using FE-SEM (XL-30S FEG, Philips Co., The Netherlands) to examine whether the shearing defect distribution was similar.

Stretch-Flangeability Evaluation Using Standard- and Small-Scale HET

isoHETs were conducted using an Erichsen hydraulic universal sheet metal testing machine (model 145-60, Erichsen Co., Germany) with 60° conical punch to evaluate the HER of the specimens in accordance with the ISO standard procedure.⁹

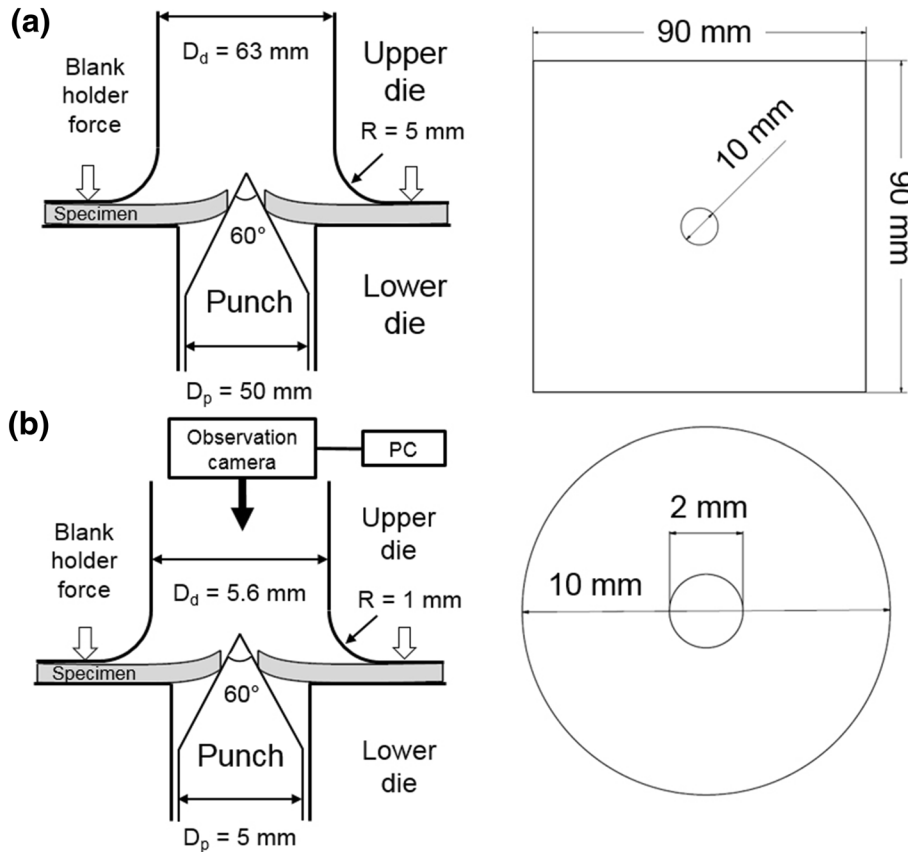


Fig. 1. Schematics of (a) isoHET and (b) pssHET system, and dimensions of HET specimen on each scale.

isoHETs were conducted at constant punch speed of 10 mm/min with constant blank holder force of 200 kN to restrict specimen slippage.

pssHETs were conducted using a universal testing machine (UTM, model RB302, R&B Co., Republic of Korea) equipped with a pssHET system. pssHETs were carried out at constant punch speed of 1.0 mm/min with constant blank holder force sufficient to prevent specimen slippage. The schematics of the isoHET and pssHET systems are shown in Fig. 1, along with the specimen dimensions.

HETs were stopped when the main crack in the hole-edge region fully propagated throughout the thickness direction. The final hole diameters were measured after the HETs. The HER was calculated using the same equation for both HETs:⁹

$$\text{HER} (\%) = \frac{d_f - d_0}{d_0} \times 100 \quad (4)$$

where d_0 and d_f are the initial and final hole diameter, respectively. In this study, the HER is an average value determined after three HETs of each specimen at each scale.

RESULTS AND DISCUSSION

Verification of Similarity of Deformation Behavior Results Between the HET Systems

In Fig. 2, “Inner” means the bottom area under the hole-edge region where the specimen directly contacts the punch, “Middle” means the central area under the hole-edge region, and “Outer” means the side opposite the “Inner” area. Each area of the specimen is shown schematically in Fig. 2b and d. Figure 2 shows the dispersion of stress triaxiality and strain as a function of HER in the hole-edge region during the pssHET and isoHET. During the HETs at both scales, Fig. 2a and c illustrates that the hole-edge region is a tensile-dominant deformation region. Furthermore, in Fig. 2b and d, the distribution of stress triaxiality for both was nearly 0.35, indicating that the deformation behavior during the HET at both scales was similar to the results of uniaxial tensile tests.¹³ The overall equivalent plastic strain and stress triaxiality distribution are shown in Supplementary Fig. S-1.

Note that, in the early stage of HET deformation (HER < 20%), the stress triaxiality in the Inner region of the pssHET sample was slightly different

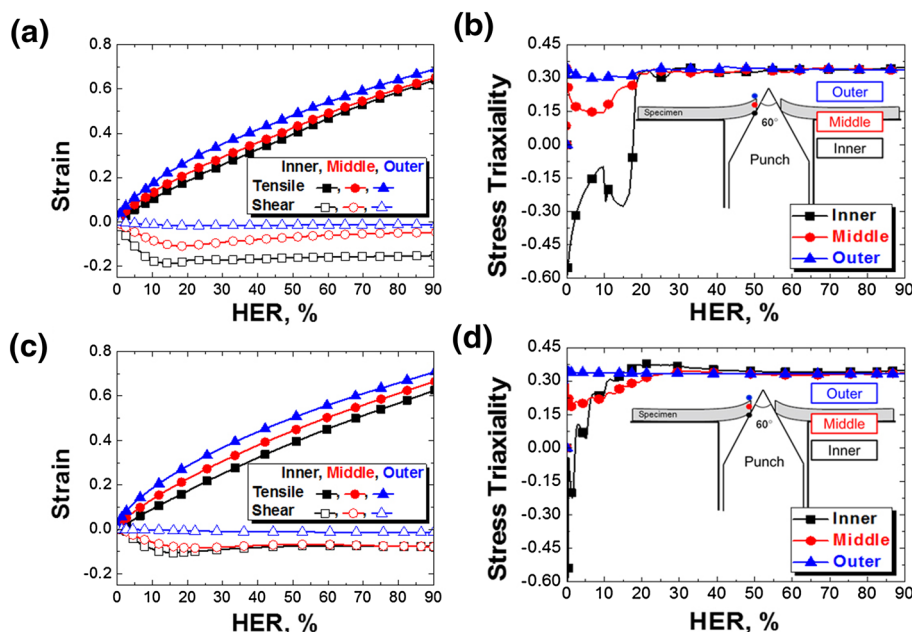


Fig. 2. Deformation behavior of (a and b) isoHET specimen and (c and d) pssHET specimen according to HER of TWIP1100 (Color figure online).

from that of the isoHET. This is because of the difference in the initial contact behavior between the hole-expansion punch and HET specimen. However, this difference between the initial compressive deformation of the pssHET and isoHET had no critical effect on the overall fracture behavior. This is because fracture initiates from the Outer region during the HET, and the deformation behavior in that region is almost the same for the HETs at both scales. Furthermore, the stress triaxiality of the Inner region of the pssHET is also similar to that of the isoHET in the $HER > 20\%$ section, where most metallic materials rupture. Thus, the overall deformation behavior results of the pssHET can be considered to be the same as those of the isoHET.

Distribution of Shearing Defects in the Initial Hole-Edge Region

In previous studies, it was reported that the HERs of the same metallic material differed depending on the initial hole-processing method.^{14–16} This is because, depending on the initial hole-processing method, the initial defect morphology and distribution in the hole-edge region were different even for the same material. In general, materials with fewer shearing defects (e.g., microcracks, microvoids, and roughness) in the initial hole-edge region showed superior HERs.¹⁷ That is, shearing defects in the initial hole-edge region have a significant effect on the HER.

It was also necessary to verify that the morphology and distribution of shearing defects of the pssHET and isoHET specimens showed similar tendencies. Figure 3a, b, f, and g shows the overall

initial hole-edge region of the TWIP1100 isoHET specimen and pssHET specimen, respectively (both fabricated using a punching process). Figure 3c–e and h–j illustrates the Inner, Middle, and Outer regions, respectively, shown in Fig. 2b, and d. The Inner regions of the HET specimens at both scales are sheared cleanly, with few microvoids or microcracks. On the other hand, the Middle and Outer regions of the HET specimens at both scales show many dimples and microvoids after shearing. It can be seen that the HET specimens at both scales show similar morphology and distribution of shearing defects in each region.

In previous study on the shearing process, the sheared surface layers were usually classified into the rollover zone, burnished zone, and fracture zone.¹⁸ The classification criteria for the sheared surface layers used in this study were the same as those of the previous study, and the shearing surface layer of the HET specimen was classified so that the rollover zone is blue, the burnished zone is yellow, and the fracture zone is red, as shown in Fig. 3b and g. The length and ratio of the shearing surface layer of each HET specimen were measured from SEM micrographs, and the results are summarized in Table S-1. The shearing surface layer ratios for the pssHET specimen were similar to those for the isoHET specimen. Thus, the shearing defect characteristics of the hole-edge region introduced during the punching process are similar in the two HET specimens at both scales, and there will be hardly any difference in the HERs of the same material due to the shearing defect characteristics as indicated by this evaluation at either HET scale.

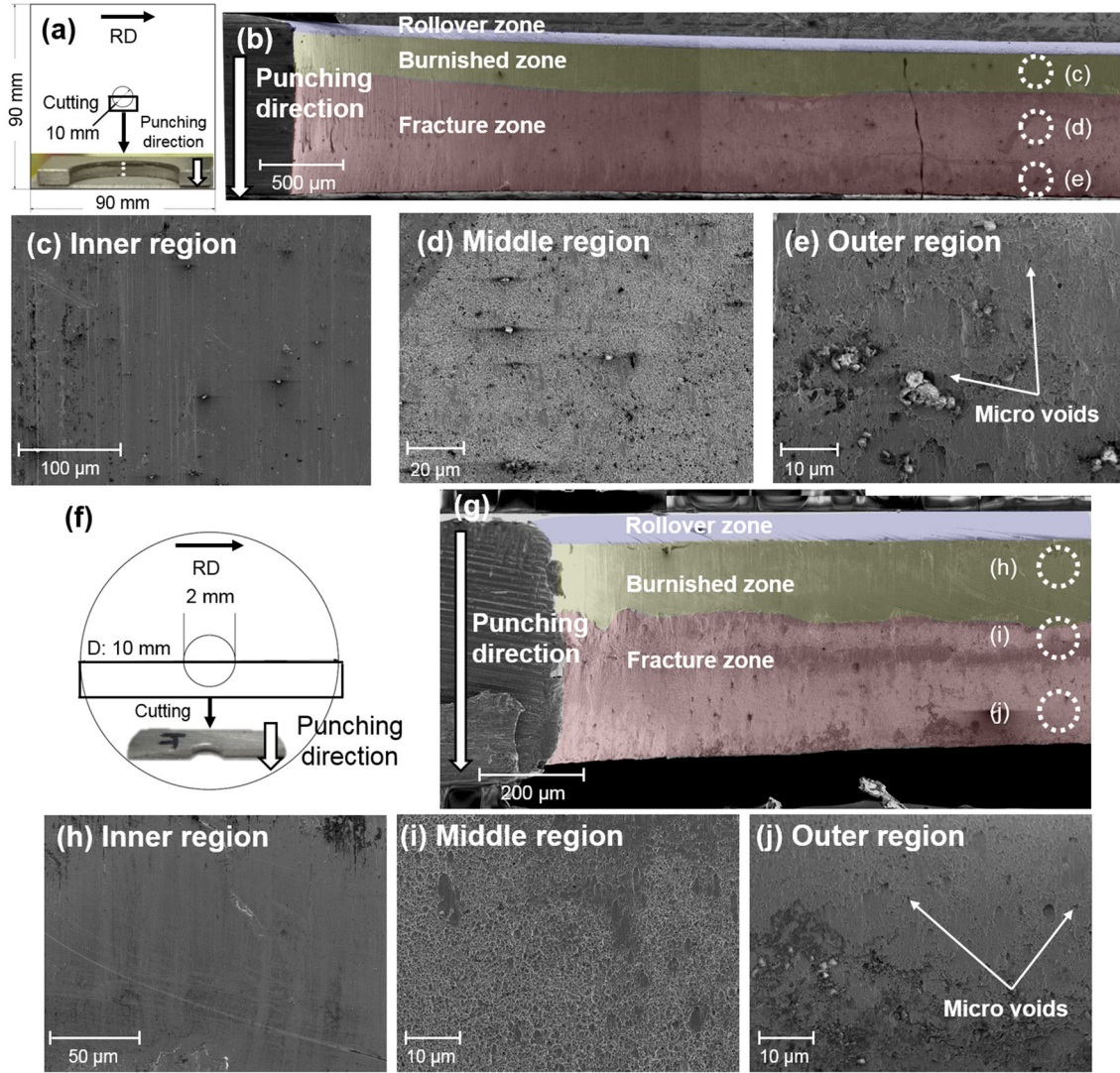


Fig. 3. SEM micrographs of initial hole-edge region of TWIP1100 (a–e) isoHET specimen and (f–j) pssHET specimen fabricated using a punching process (Color figure online).

Stretch-Flangeability Evaluation Results of Small- and Standard-Scale HET

It was found that stretch-flangeability evaluation of the four kinds of AHSS provided the same levels of HER results using HETs on both scales, as summarized in Table I. The reasons that the same level of HER results were obtained in the isoHET system and pssHET system are (1) the HET deformation behavior was similar at both scales, (2) the morphology and distribution of shearing defects introduced when the initial hole of each HET specimen was machined using the punch process were identical in pssHET and isoHET specimens, and (3) the pssHET specimens used in this study did not have a grain-size effect, which might change their mechanical properties. This is because the AHSS grain sizes are between 1 μm and 10 μm, while the thickness of the pssHET specimen is at least 50 times larger.

Table I. Results of isoHET and pssHET for AHSS specimens

Specimen	HER of pssHET (%)	HER of isoHET (%)
TWIP1100	31.63 ± 1.20	31.97 ± 3.37
DP980	30.96 ± 0.80	30.04 ± 2.43
DP780	28.92 ± 0.57	27.85 ± 0.53
TRIP780	22.65 ± 1.38	23.95 ± 1.49

We propose herein a new method for measuring the stretch-flangeability of metallic materials using a smaller-scale HET system. The advantages of this small-scale method are that it can reliably measure the stretch-flangeability of metallic materials using a small amount of specimen, and thus that the

stretch-flangeability can be measured even in a localized area. The newly developed small-scale HET system can be used to evaluate quickly and accurately the stretch-flangeability of steel types under development (or consideration) and to provide feedback. In addition, when it is necessary to evaluate the stretch-flangeability of an existing metallic material, the newly developed small-scale HET system is more economical because it can measure stretch-flangeability with a smaller amount of test specimen.

CONCLUSION

A small-scale HET system for evaluating the stretch-flangeability with small specimens was developed. The results from the pssHET system were compared those from the isoHET system, and it was verified that the evaluation of stretch-flangeability using the new HET system provided high reproducibility and reliability. The following conclusions can be drawn from the results of this study:

1. The deformation behavior of the pssHET system was analyzed using FEM. Based on strain and stress triaxiality analysis around the hole-edge region, the deformation behavior of the pssHET and isoHET was found to be similar.
2. The morphology and distribution of shearing defects in the hole-edge region, introduced when the initial hole of the HET specimen was made during the punching process, played significant roles in the HET. SEM results for defects of the shearing surface in the hole-edge region of the pssHET and isoHET specimens were similar.
3. The stretch-flangeability of various types of AHSS was evaluated using the isoHET and pssHET systems. Reproducible results were obtained with the pssHET, and the same level of HER results was obtained compared with the isoHET. We verified the reliability of the proposed method.

ACKNOWLEDGEMENTS

This work was supported by a National Research Foundation of Korea (NRF) Grant funded by the Korea government (MSIP) (No. 2014R1A2A1A100 51322). This study was supported by the Brain

Korea 21 PLUS Project for the Center for Creative Industrial Materials (F16SN25D1706).

CONFLICT OF INTEREST

The authors declare that they have no conflict of interest.

ELECTRONIC SUPPLEMENTARY MATERIAL

The online version of this article (<https://doi.org/10.1007/s11837-018-2766-7>) contains supplementary material, which is available to authorized users.

REFERENCES

1. M. Ma and H. Yi, *Advanced Steels*, ed. Y. Weng, H. Dong, and Y. Gan (Berlin: Springer, 2011), p. 187.
2. O. Bouaziz, H. Zurob, and M. Huang, *Steel Res. Int.* 84, 937 (2013).
3. S.-Y. Lee, S.-I. Lee, and B. Hwang, *Korean J. Met. Mater.* 54, 637 (2016).
4. E.-Y. Kim, S.I. Kim, and S.-H. Choi, *Korean J. Met. Mater.* 54, 808 (2016).
5. H.W. Lee, M.H. Cha, B.K. Choi, G.S. Kim, S.H. Park, and A.I.P. Conf, *Proceedings* 1383, 48 (2011).
6. X. Chen, H. Jiang, Z. Cui, C. Lian, and C. Lu, *Proc. Eng.* 81, 718 (2014).
7. J.I. Yoon, J. Jung, J.G. Kim, S.S. Sohn, S. Lee, and H.S. Kim, *J. Mater. Sci.* 52, 7808 (2017).
8. G. Jha, S. Das, A. Lodh, and A. Haldar, *Mater. Sci. Eng. A* 552, 457 (2012).
9. ISO, Metallic materials—method of hole expanding test (ISO, 2017), <https://www.iso.org/standard/69771.html>. Accessed 12 December 2017.
10. R. Ben Hmida, S. Thibaud, A. Gilbin, and F. Richard, *Mater. Des.* 45, 155 (2013).
11. Z.T. Xu, L.F. Peng, M.W. Fu, and X.M. Lai, *Int. J. Plast* 68, 34 (2015).
12. M.W. Fu and W.L. Chan, *Mater. Des.* 32, 4738 (2011).
13. Y. Bai and T. Wierzbicki, *Int. J. Fract.* 161, 1 (2010).
14. J.I. Yoon, J. Jung, H.H. Lee, G.-S. Kim, and H.S. Kim, *Met. Mater. Int.* 22, 1009 (2016).
15. J.I. Yoon, J. Jung, S.-H. Joo, T.J. Song, K.-G. Chin, M.H. Seo, S.-J. Kim, S. Lee, and H.S. Kim, *Mater. Lett.* 180, 322 (2016).
16. K. Hasegawa, K. Kawamura, T. Urabe, and Y. Hosoya, *ISIJ Int.* 44, 603 (2004).
17. J.I. Yoon, J. Jung, J.H. Ryu, K. Lee, and H.S. Kim, *Exp. Mech.* 57, 1349 (2017).
18. K.-I. Mori, Y. Abe, and Y. Suzui, *J. Mater. Process. Technol.* 210, 653 (2010).